09

Analytical model for calculating the spatial resolution of 2D IR photodiode arrays with small pixel size

© V.V. Vasiliev, A.V. Vishnyakov, V.A. Stuchinsky

Rzhanov Institute of Semiconductor Physics, Russian Academy of Sciences, Siberian Division,
630090 Novosibirsk, Russia
e-mail: vas@isp.nsc.ru

Received March 24, 2025
Revised June 9, 2025
Accepted June 9, 2025

An analytical model is proposed to describe the spatial resolution of 2D IR photodiode arrays with a diode-size value close to the pixel size. The model allows one to analyze the important case of diode arrays with small pixel sizes and an arbitrary ratio of the latter to the diffusion length of charge carriers and to the absorber-layer thickness. In addition to the standard Sinc-multiplier, the expression for the modulation transfer function of the analyzed diode arrays includes a factor that describes the deviation from the Sinc-multiplier, this deviation increasing with spatial frequency. The effect due to the additional factor becomes more appreciable with decreasing the array pitch and/or with increasing the photosensitive-layer thickness. A quantitative comparison of calculations within the proposed model with the calculations using the Monte Carlo method for modeling the diffusion of photogenerated charge carriers is performed.

Keywords: analytical model, 2D IR detector, spatial resolution, Nyquist frequency, line spread function, modulation transfer function.

DOI: 10.61011/TP.2025.11.62244.44-25

Introduction

Besides the desired limitation of infrared (IR) photodetector arrays in the focal plane when the focal-plane-array format is increased, the existing trend towards the reduction of pixel size of such arrays is caused by the need for increasing the spatial resolution of photodetectors (PD) [1,2]. When the size of array used for imaging is fixed, the only way to increase the sampling density and the spatial resolution is to decrease the pixel size. However, a decrease in array photodetector (APD) sensitivity is an undesired result of pixel size reduction [3,4]. Array pixel size in such conditions shall be chosen through a tradeoff between the achievable spatial resolution of PD and its sensitivity. Since this tradeoff shall be achieved in conditions involving interaction of various system components, full system simulation of such devices is used for APD optimization [4]. As for technological constraints imposed on photodetector structure parameters, it should be emphasized that, for example, modern APD technology based on cadmium-mercury-tellurium (CdHgTe) material provides arrays with a pixel size smaller than 10 and even $5\,\mu$m for a long-wavelength IR range [5].

There are many theoretical and experimental studies focused on the effect of structural parameters of photodetector arrays (such as array pitch, lateral diode size, and photosensitive layer thickness) on the spatial resolution provided by photodetectors (see, for example, [6–9]). Studies [6,7,10] and some other works investigated the influence of array pitch on the modulation transfer function (MTF) of the array [11], and it was shown that an increase in array resolution took place when passing to arrays with a smaller pixel size at spatial frequencies approximately equal to Nyquist frequency f_N.

Degradation of IR photodetector array resolution with growth of the photosensitive layer thickness has been numerically studied earlier (for CdHgTe-based APD) in [8,9] and observed experimentally (for InSb-based APD) in [12]. The reasons for this decrease in resolution are in lateral scattering of photogenerated charge carriers (PCCs) from the places where they were produced, that occurs as these charge carriers (CCs) diffuse across the photosensitive material layer until running onto diodes. The thicker the photosensitive layer the farther apart the photocarriers are scattered. As a result, a central portion with a weakly varying signal is formed on the line-spread function (LSF) [11]. The width of this portion is one of the parameters defining the spatial resolution of the array [6,7,10]. The rate of LSF decay at the side slopes of this function is another parameter defining the array resolution. It is defined by the effective length of PCC diffusion [8].

Besides numerical simulation, analytical models (AMs) are often used to describe the spatial resolution of IR array photodetectors (PD) due to the simplicity and clarity of AMs. Supplementing the numerical computation, an AM also has its inherent value because it often ensures a better understanding of processes defining IR PD operation. Therefore, computations are sometimes accompanied with AM development.

If the real photosensitivity of APD pixels is approximated by a stepped profile with a width equal to the array pitch Δ, then the corresponding array modulation transfer function

will be equal to

$$\mathrm{MTF}(f) = \frac{\int\limits_{-\Delta/2}^{\Delta/2} e^{2\pi i f x} dx}{\Delta} = \frac{\sin(\pi f \Delta)}{\pi f \Delta}, \qquad (1)$$

where f is the spatial frequency. With $f_N = (2\Delta)^{-1}$, equation (1) gives $\mathrm{MTF}(f_N) = 2/\pi \approx 0.636$. This equation known in the literature as a footprint approximation provides an important and commonly used reference standard for comparing the resolution of different PDs [13]. However, this standard contains only one photodetector array parameter — Δ, and therefore is hardly suitable for describing real photodetector arrays, whose resolution can differ from that given by equation (1). Thus, for example, as the array pitch decreases from 30 to 15 μm, the resolution at Nyquist frequency may be lower than the values predicted by equation (1) [6,7]. Such resolution degradation taking place when the array dimensions and/or diffusion length vary may be attributed to scaling violation as the pixel sizes decrease. Actually, as it follows from the analysis of continuity equation for photocarriers (see equation (2) below), if all dimensions in the problem, including photocarrier diffusion length, optical absorption length, etc., are reduced by half, then the resolution at Nyquist frequency will remain unchanged; however, the Nyquist frequency will double. Photosensitive layer thickness, charge carrier diffusion length in the photosensitive material and lateral sizes of array diodes are the main variables that infringe scaling.

The purpose of this study was to derive an analytical equation for IR photodetector array resolution, which is similar to equation (1) yet considers deviations from the latter at a small array pitch or larger photosensitive layer thickness. Within the analytical model, we restrict ourselves to the lateral photodiode size W equal to Δ. Array MTF may be precisely calculated in this case. Relation between all other photodetector parameters is arbitrary. Thus, the model is relevant to arrays with small pixel size and arbitrary relation between the pixel size and charge carrier diffusion length and photosensitive layer thickness. Moreover, the deepening of p-n junctions of photodiodes into the photosensitive film was assumed equal to zero for clarity in this study. In this case, photocarrier concentration on the $y = d$ surface (Figure 1) is equal to zero; such simple boundary condition is used to calculate MTF without additional simplifying assumptions as function of pixel size, photosensitive layer thickness and IR radiation absorption coefficient.

Besides the analytical simulation, we also performed numerical simulation of the array resolution using the Monte Carlo (MC) method used for CC diffusion simulation in the photosensitive layer [8]. The objective of numerical simulation was to identify the resolution variations induced by the difference between the diode size and pixel size. The array parameter values used the simulation of photocarrier diffusion by the MC method and for the analysis of the analytical model were coinsident with one another, except for the diode size W in the MC calculation, which could be a little smaller than the pixel size specified in this work.

1. Mathematical model formulation and calculation results

Consider an MTF measurement procedure for IR photodetector arrays with inverse exposure geometry (Figure 1). After production, photogenerated charge carriers diffuse laterally from an infinitely narrow and infinitely long illumination spot, partially recombining over the diffusion length L_d; and the farther from the illumination spot they move, the greater becomes the size of the photocarrier distribution region along the X axis. Thus, if the film thickness d is small, and the spot-scan profile, or LSF, is near-rectangular, then, as the thickness d increases, the LSF fronts will become more gently sloping due to photocarrier diffusion.

LSF may be represented as an infinite series of alternating-sign photocarrier source images chosen to meet the following boundary conditions: zero concentration of photocarriers at $y = d$ and zero value of the normal current component $y = 0$. MTF may be calculated by means of the Fourier transform of the found MTF, for which rather a complicated problem shall be solved. However, MTF may be found more easily by solving a problem for Fourier harmonics of a signal. Specifically, calculate photodiode current during array exposure to radiation with intensity distribution $C \cdot \exp(2\pi i f x)$ and spatial frequency f (here, the exposure amplitude C is constant and independent of f). The found photosignal normalized to unity at $f = 0$ is the desired MTF. Multiple reflections of IR radiation from the film boundaries are neglected for clarity; then the continuity equation for photocarriers is written as

$$\Delta n - \frac{n}{L_d^2} + \frac{g_0}{D} \exp(-\alpha y + ikx) = 0. \qquad (2)$$

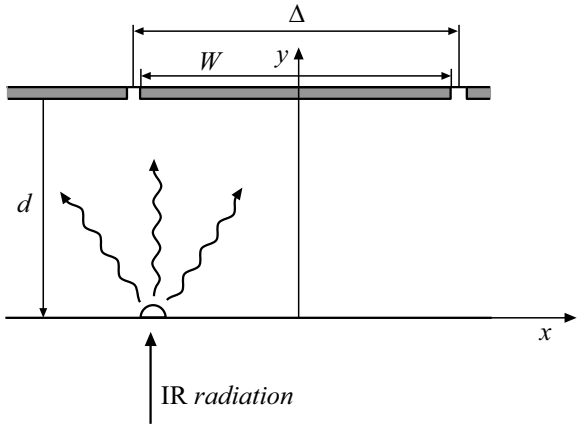

Figure 1. Measurement of array MTF in inverse exposure geometry. Δ — array pitch, $W \approx \Delta$ — diode size, d — photosensitive layer thickness. Linear illumination spot extends along the z axis perpendicular to the pattern plane.

Hereinafter, $k = 2\pi f$ is the wave vector, D is the CC diffusion constant, L_d is the PCC diffusion length, α is the IR radiation absorption coefficient, g_0 is the generation rate of photocarriers on the $y = 0$ surface independent of f. Particular solution of equation (2) is found as $n = \beta \cdot \exp(-\alpha y + ikx)$. Substituting the last expression into equation (2), we get $\beta = g_0 \cdot D^{-1}[L^{-2}(k) - \alpha^2]^{-1}$, where $L(k)$ satisfies

$$L^{-2}(k) = L_d^{-2} + k^2. \tag{3}$$

General solution of the equation (2) is written as

$$\left[\beta \exp(-\alpha y) + A \exp\left(-\frac{y}{L(k)}\right) + B \exp\left(\frac{y}{L(k)}\right)\right] \exp(ikx).$$

Substituting this expression into the boundary conditions $n(x, y = d) = 0$ and $\frac{\partial n}{\partial y}[x, y = 0] = 0$, we obtain the following two linear equations with respect to A and B:

$$B \exp(-\alpha d) + A \exp\left(-\frac{d}{L(k)}\right) + B \exp\left(\frac{d}{L(k)}\right) = 0,$$

$$-\alpha\beta - \frac{A}{L(k)} + \frac{B}{L(k)} = 0.$$

Finding A and B from these equations, we have

$$A = -\beta \frac{e^{-\alpha d} + \alpha L(k) e^{\frac{d}{L(k)}}}{2ch\left(\frac{d}{L(k)}\right)},$$

$$B = -\beta \frac{e^{-\alpha d} - \alpha L(k) e^{\frac{d}{L(k)}}}{2ch\left(\frac{d}{L(k)}\right)}.$$

The current flowing through the diode is expressed as

$$I(k) = -D\Delta \int_{-\Delta/2}^{\Delta/2} \frac{\partial n}{\partial y}[x, y = d]dx = \frac{2D\Delta \sin(k\Delta/2)}{k}$$

$$\times \left[\alpha\beta \cdot \exp(-\alpha d) + \frac{A \cdot \exp\left(-\frac{d}{L(k)}\right)}{L(k)} - \frac{B \cdot \exp\left(\frac{d}{L(k)}\right)}{L(k)}\right].$$

Substituting here the expressions for A and B, we get

$$I(k) = \frac{g_0 \Delta^2 \alpha}{\left(\alpha^2 - \frac{1}{L^2(k)}\right)} \left[\frac{1}{ch(\frac{d}{L(k)})} - e^{-ad} \times \left(1 + \frac{th\left(\frac{d}{L(k)}\right)}{\alpha L(k)}\right)\right] \mathrm{Sinc}(k\Delta/2), \tag{4}$$

where $\mathrm{Sinc}(x) = \sin(x)/x$. Note that though the denominator in (4) vanishes at $\alpha L(k) = 1$, expression (4) has no singularity at this point. The desired $\mathrm{MTF}(k)$ is equal to $I(k)/I(0)$, giving

$$\mathrm{MTF}(k) = \frac{\left(\alpha^2 - \frac{1}{L_d^2}\right)}{\left(\alpha^2 - \frac{1}{L^2(k)}\right)} \frac{\left[\frac{1}{ch\left(\frac{d}{L(k)}\right)} - e^{-\alpha d}\left(1 + \frac{th\left(\frac{d}{L(k)}\right)}{\alpha L(k)}\right)\right]}{\left[\frac{1}{ch\left(\frac{d}{L_d}\right)} - e^{-\alpha d}\left(1 + \frac{th\left(\frac{d}{L_d}\right)}{\alpha L_d}\right)\right]} \times \mathrm{Sinc}(k\Delta/2). \tag{5}$$

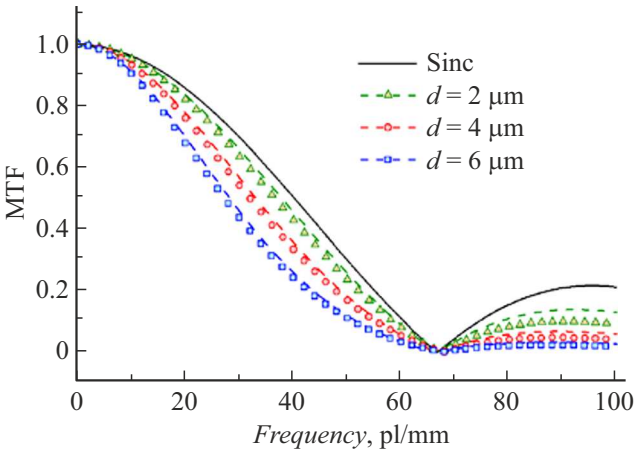

Figure 2. MTFs of photodetector arrays calculated using the MC method for CC diffusion analysis and MTFs of the same arrays calculated using equation (5) (symbols and lines, respectively). CC diffusion length — 10 μm, IR radiation absorption depth — 2 μm, photosensitive layer thicknesses — 2, 4 and, 6 μm. The black line shows $\mathrm{Sinc}(\pi f \Delta)$ calculated using equation (1) with $\Delta = 15\,\mu$m. The diode size in the MC calculation is 12 μm.

For three film thicknesses d, Figure 2 shows the MTFs of photodetector arrays for $L_d = 10\,\mu$m calculated using equation (5), and the MTFs calculated using the MC method for PCC diffusion analysis. Data obtained using equation (1) are also shown. Hereinafter, lines show AM curves, and symbols show the data calculated using the MC method. MC calculation data substituted in Figure 2 were obtained for arrays with 12 μm diodes. MC calculation data for a diode size equal to the array pitch of 15 μm coincide with the AM data and are not shown for clarity. The difference between the lines and symbols shows the design decrease in MTF as the diode size decreases from 15 to 12 μm.

It can be seen that in line with the afore-said, the resolution degrades as the thickness d grows. It can be also seen that the MC calculation yields gives slightly lower resolutions than those of AM; this is due to smaller diodes treated in the MC calculation.

Figure 3 shows the MTFs of photodetector arrays calculated using AM (equation (5)) and the MTSs of photodetector arrays calculated using the MC method for arrays with a 6 μm photosensitive layer and CC bulk diffusion lengths of 3, 5, and 20 μm. It can be seen that,

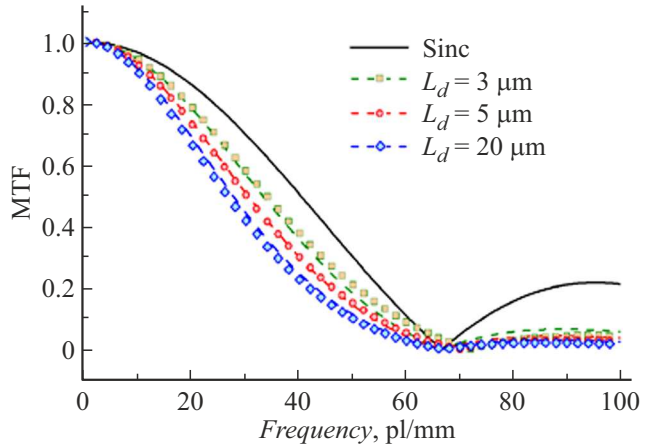

Figure 3. MTFs of photodetector arrays with 6 μm photosensitive layer and CC diffusion lengths of 3, 5 and 20 μm calculated using the MC method, and MTFs of the same arrays calculated using equation (5) (symbols and lines, respectively), $\alpha = 0.5\,\mu\text{m}^{-1}$, $\Delta = 15\,\mu$m. The black line shows $\text{Sinc}(\pi f \Delta)$. The diode size in the MC calculation is 12 μm.

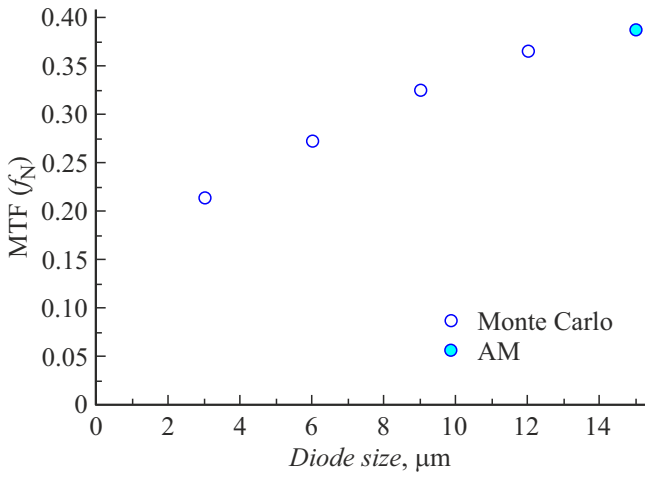

Figure 4. MIT values at Nyquist frequency calculated using the MC method and analytical model (equation (5)) as dependent on the lateral photodiode sizes (empty circles and solid circle, respectively). Parameter values: $d = 6\,\mu$m, $L_d = 10\,\mu$m, $\alpha = 0.5\,\mu\text{m}^{-1}$, $\Delta = 15\,\mu$m.

as the diffusion length decreases, the resolution improves, approaching that given by equation (1). The difference in MTF at Nyquist frequency (33 lines/mm) between the MTF values shown with symbols and lines is in total max. 7% of that of Figures 2 and 3, while the diode size W varies by $(15-12)/15 = 20\,\%$.

Figure 4 shows MTF values at Nyquist frequency calculated using the MC method and equation (5) versus the lateral photodiode sizes (empty circles and a solid circle, respectively). The following parameter values were adopted in the calculation: $d = 6\,\mu$m, $L_d = 10\,\mu$m, $\alpha = 0.5\,\mu\text{m}^{-1}$, $\Delta = 15\,\mu$m. It can be seen that the AM data for 15 μm diodes and MC data for arrays with smaller diodes form a smooth dependence. Note here that for arrays with smaller diodes (much smaller than the pixel size), the AM for obvious reasons is inapplicable.

Consider the case of a small optical absorption length $l_{opt} = \alpha^{-1}$. Assuming that in (5), we have:

$$\text{MTF}_{l_{opt}=0}(k) = \frac{ch\left(\frac{d}{L_d}\right)}{ch\left(\frac{d}{L(k)}\right)}\text{Sinc}(k\Delta/2). \qquad (6)$$

Note that equation (6) may be also derived if the bulk generation of excess CC is set to zero and a boundary condition for CCs generation on the $y = 0$ surface is introduced instead of it: $j_y(y=0) = j_0\exp(ikx)$, where the current density due to CC surface generation j_0 is independent of frequency. Then the solution will be written as $n = \frac{j_0 L(k)}{Dch\left(\frac{d}{L(k)}\right)} e^{ikx} sh\left(\frac{d-y}{L(k)}\right)$. The diode current is equal to $\frac{j_0\Delta^2\text{Sinc}(k\Delta/2)}{ch\left(\frac{d}{L(k)}\right)}$. Hence, equation (6) is derived again.

Besides the ordinary Sinc function, the $ch(d\cdot L_d^{-1})\cdot\left[ch(d\cdot L^{-1}(k))\right]^{-1}$ multiplier arises in expression (6). This multiplier arises due to the following fact: solutions of equation (2) written as $\exp(ikx - y/L(k))$ decay by e times at a depth of $L(k)$, which, owing to relation (3), depends on the spatial frequency f. As f grows in value, the function $L(k)$ decreases; consequently, the signal modulation on the photodiode surface decreases in proportion to $\exp(-d/L(k))$, i.e. the resolution is degraded. The effect due to this additional multiplier is higher at small array pitch values (i.e. at higher spatial frequencies) and large photosensitive layer thicknesses. Therefore, the proposed analytical model is particularly important for arrays with a small pixel size.

With $L_d \to \infty$ expression (3) reduces to $\frac{1}{L(k)} = k$, and in this case the LSF can be derived from expression (6) for MTF by the inverse Fourier transform using the fact that $\int\limits_{\infty}^{-\infty} \frac{\exp(-ikx)}{ch(kd)}\,dk = \frac{\pi}{dch\left(\frac{\pi x}{2d}\right)}$. A convolution in LSF corresponds to the multiplication of multipliers in MTF; in the given Sinc case, the convolution corresponds to integration from $(x-\Delta/2)$ to $(x+\Delta/2)$. Then we obtain:

$$\text{LSF}_{l_{opt}=0,L_d\to\infty}(x) \approx \frac{\pi}{d}\int\limits_{x-\Delta/2}^{x+\Delta/2}\frac{dz}{ch\left(\frac{\pi\cdot z}{2d}\right)}$$

$$\approx \frac{2}{\pi}[\arctan(\exp((\pi\cdot(x+\Delta/2))/(2d)))$$

$$-\arctan(\exp((\pi\cdot(x-\Delta/2))/(2d)))]. \qquad (7)$$

Here, the normalization multiplier $2/\pi$ is chosen such that the signal be equal to unity at the center of the pixel far from its edges. Figure 5 shows the LSF curve (7) for $d = 3$, and the LSF obtained by MC calculations for the same values of parameters except for W, for which the value of 12 μm was

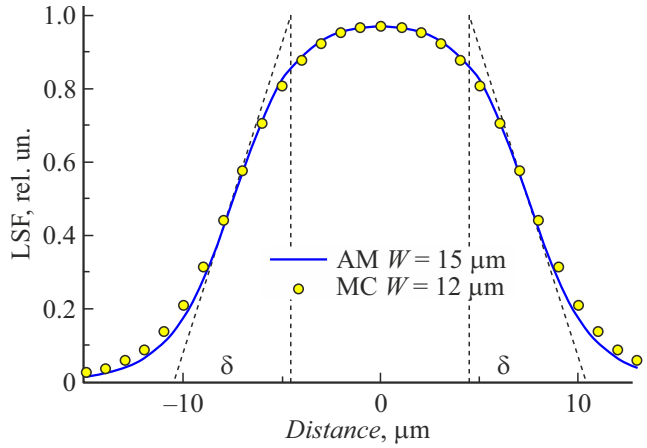

Figure 5. LSF according to the analytical model (equation (7)) and LSF calculated using the MC method (the line and symbols, respectively). Adopted parameter values: $d = 3\,\mu$m, $L_d = \infty$, $l_{opt} = 0$, $\Delta = 15\,\mu$m. The diode size in the MC calculation is $12\,\mu$m. The width δ of the LSF decay region is indicated.

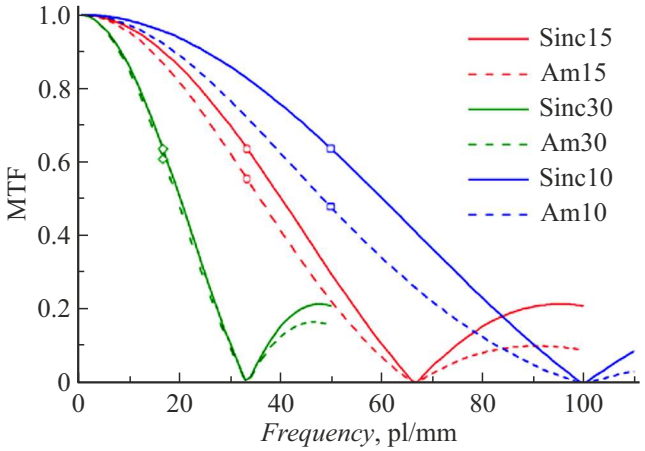

Figure 6. Solid curves — MTFs calculated using equation (1) for arrays with a pitch of $\Delta = 30$, 15 and $10\,\mu$m (green, red and blue lines, respectively). Dashed curves — MTFs calculated using the analytical model (equation (5)) for the same pitch values. Large symbols show the MTF values at Nyquist frequency. Parameter values: $d = 3\,\mu$m, $L_d = 10\,\mu$m, $l_{opt} = 2\,\mu$m.

adopted. It can be seen that both calculation methods yield nearly identical LSF curves; however, for $W = 12\,\mu$m the MC calculation shows a slight decay broadening, which can be attributed to the presence of a gap between the edges of adjacent diodes.

As it follows from (7) and shown in Figure 5, the width δ of the decay region of such an analytical LSF as determined from the slope of the signal at points $x = \pm\Delta/2$ is equal to $2d$. Away from the pixel, the signal decays as $(2/\pi) \cdot \exp(-\pi(|x| - \Delta/2)/(2d))$. As the film thickness d increases in value or the diode pitch Δ decreases, the deviation of the LSF shape from a rectangle will become more pronounced.

Consider expression (7) as a sum of contributions photocarrier source images. At $L_d \to \infty$, there is no bulk recombination of photocarriers in the film, and the contribution of each image to the diode current in this case will vary in proportion to the solid angle at which the diode is seen from the location of the source image. Then the total signal due to all images will be equal to $\frac{2}{\pi}\sum_{n-0}^{\infty}(-1)^n\left(\arctan\left(\frac{\Delta/2+x}{d+2nd}\right)+\left(\frac{\Delta/2-x}{d+2nd}\right)\right)$. The sum of this series converges to (7), which fact can be proved by summing a sufficiently large number of terms of the series and comparing the result with that calculated by expression (7). Near the center of pixel, the first term of the series is sufficient, like in the case of the analytical model of [14], because the contributions due to more remote source images partially compensate each other and induce sharper edge decays of LSF.

Figure 6 shows MTFs calculated using equation (1) and equation (5) for arrays with a pitch of 30, 15 and $10\,\mu$m. It can be seen that there is a difference between the footprint approximation and AM predictions growing as the array pitch decreases. This difference starts manifesting itself with decreasing pixel sizes when the doubled value of δ turns out to be comparable with the pixel size. Therefore, the critical pixel size below which the violation of the footprint approximation shall be expected, may be estimated from Figures 5 and 6 as equal to $4d$. For a film thickness of $3\,\mu$m (Figure 6), this size is approximately equal to $2\,\mu$m. For maintaining the spatial resolution with decreasing array pitch, the photosensitive layer thickness shall be reduced.

Conclusion

An analytical model describing the spatial resolution of IR photodetector arrays with the lateral diode sizes close to the pixel size was proposed. The MTF of such model structure is easily calculated (see equation (5)). Besides the known $\mathrm{Sinc}(f)$ function corresponding to the footprint approximation for pixel sensitivity to radiation [13], the derived equation involves an additional multiplier describing the degradation of spatial resolution at Nyquist frequency compared with the footprint approximation. This degradation becomes more pronounced as the array pitch decreases and/or the photosensitive layer thickness (or CC diffusion length) increases. In case of a large diffusion length and radiation absorption coefficient, a simple formula for the LSF of the given arrays can be also in addition to the formula for MTF. Comparison of AM data with the MC calculation shows that when the diode sizes differ from the pixel size within 20 %, the difference in MTF values is max. 7 %.

Conflict of interest

The authors declare no conflict of interest.

References

[1] A. Rogalski, P. Martyniuk, M. Kopytko. Rep. Prog. Phys., **79**, 046501 (2016). DOI: 10.1088/0034-4885/79/4/046501

[2] R.G. Driggers, R.H. Vollmerhausen, J.P. Reynolds, J.D. Fanning, G.C. Holst. Opt. Engineer., **51** (6), 063202 (2012). DOI: 10.1117/1.OE.51.6.063202

[3] N.K. Dhar, R. Dat, A.K. Sood. *Advances in Infrared Detector Array Technology*, p. 182, Chapter 7 in S.L. Pyshkin, J. Ballato (editors). *Optoelectronics — Advanced Materials and Devices* (InTech., 2013), p. 149–190. DOI: 10.5772/51665

[4] J. Farrell, F. Xiao, S. Kavusi. *Resolution and light sensitivity tradeoff with pixel size*, Proc. of Electronic Imaging Conference (San Jose, California, United States, 2006), v. 6069, Digital Photography II; 60690N (2006). DOI: 10.1117/12.646805

[5] W.E. Tennant, D.J. Gulbransen, A. Roll, M. Carmody, D. Edwall, A. Julius, P. Dreiske, A. Chen, W. McLevige, S. Freeman, D. Lee, D.E. Cooper, E. Piquette. J. Electron. Mater., **43** (8), 3041 (2014). DOI: 10.1007/s11664-014-3192-4

[6] O. Gravrand, N. Baier, A. Ferron, F. Rochette, J. Berthoz, L. Rubaldo, R. Cluzel. J. Electron. Mater., **43** (8), 3025 (2014). DOI: 10.1007/s11664-014-3185-3

[7] J. Berthoz, R. Grille, L. Rubaldo, O. Gravrand, A. Kerlain, N. Pere-Laperne, L. Martineau, F. Chabuel, D. Leclercq. J. Electron. Mater., **44** (9), 3157 (2015). DOI: 10.1007/s11664-015-3857-7

[8] V.A. Stuchinsky, A.V. Vishnyakov, V.V. Vasiliev, J. Opt. Technol., **91** (2), 96 (2024). DOI: 10.1364/JOT.91.000096

[9] I.I. Lee, V.G. Polovinkin. IEEE Trans. on Electron. Devices, **67** (8), 3175 (2020).

[10] L. Martineau, L. Rubaldo, F. Chabuel, O. Gravrand, in: Proc. SPIE 8889, *Sensors, Systems, and Next-Generation Satellites XVII*, 88891B (2013), DOI: 10.1117/12.2028883

[11] G.D. Boreman, *Modulation transfer function in optical and electro-optical systems. Second edition.* (2021), DOI: 10.1117/3.419857

[12] K.O. Boltar, P.V. Vlasov, P.S. Lazarev, A.A. Lopukhin, V.F. Chishko. Prikladnaya fizika, **1**, 18 (2020) (in Russian).

[13] B. Appleton, T. Hubbard, A. Glasmann, E. Bellotti. Opt. Express, **26** (5), 5310 (2018). DOI: 10.1364/OE.26.005310

[14] M. Vallone, M. Goano, F. Bertazzi, G. Ghione, S. Hanna, D. Eich, H. Figgemeier, J. Electron Device Society, **6**, 664 (2018). DOI: 10.1109/JEDS.2018.2835818

Translated by E.Ilinskaya